Acta Cryst. (1967). **23**, 307

The Ordered Structure of TiO

BY D. WATANABE* AND J. R. CASTLES
School of Physics, University of Melbourne, Parkville, Victoria, Australia

AND A. JOSTSONS† AND A. S. MALIN
School of Metallurgy, University of New South Wales, Kensington, N.S.W., Australia

(*Received* 6 *October* 1966 *and in revised form* 16 *January* 1967)

The low temperature form of the phase, TiO, which is stable in the composition range $TiO_{0.9}-TiO_{1.1}$ below 990°C, has been investigated by electron microscopy/diffraction and X-ray powder methods. The unit cell is monoclinic (space group $A2/m$) with $a=5.855$, $b=9.340$, $c=4.142$ Å and $\gamma=107°32'$. The structure is similar to that of NaCl, but has an ordered array of vacant lattice sites. Half of the titanium and half of the oxygen atoms are missing alternately in every third (110) plane. Microstructural features of the ordered phase are also described and the crystallography of the ordering transformation is discussed.

1. Introduction

Many oxides, carbides and nitrides of the Group IVa and Va metals crystallize with the simple NaCl type structure at compositions of about MX. These compounds generally have wide ranges of non-stoichiometry. In particular, the phase TiO has long been known to exist over a wide range of composition depending on temperature, *e.g.* from $TiO_{0.7}$ to $TiO_{1.25}$ at 1400°C and $TiO_{0.9}$ to $TiO_{1.25}$ at temperatures below about 990°C (Hansen, 1958; Jostsons & McDougall, 1967). An important feature of this phase, which has been deduced from a comparison of pycnometric and X-ray densities (Ehrlich, 1941; Andersson, Collen, Kuylenstierna & Magnéli, 1957), is that its crystal structure has varying proportions of titanium and oxygen vacancies. At the composition $TiO_{0.7}$ the titanium lattice is almost perfect, but about a third of the oxygen sites are vacant. In $TiO_{1.25}$ the oxygen lattice is almost perfect, but about a quarter of the titanium sites are vacant. Even in the equiatomic alloy about 15% of both titanium and oxygen sites are vacant. It has been concluded from X-ray examinations (Ehrlich, 1941; Andersson, Collen, Kuylenstierna & Magnéli, 1957) that these vacancies are arranged randomly at high temperatures.

Naylor (1946) observed a discontinuity in the specific heat of TiO at 990°C indicating a phase change. Subsequently, Jenkins (1953) reported the splitting of NaCl type reflexions on the X-ray patterns from a powder sample of the equiatomic alloy annealed at 870°C. Later, some investigators (Wang & Grant, 1956; Andersson, Collen, Kruuse, Kuylenstierna, Magnéli, Pestmalis & Åsbrink, 1957; Pearson, 1958) observed a number of weak reflexions in addition to the split reflexions observed by Jenkins. Although attempts to index these extra reflexions were not successful, Andersson, Collen, Kuylenstierna & Magnéli (1957) suggested that the transformation occurring below 990°C (the equilibrium temperature) is a consequence of the ordering of vacancies.

The present paper reports the structure analysis of the low temperature form of TiO utilizing the electron microscopy/diffraction and X-ray powder methods. The main advantage of electron microscopy for studying ordered structures lies in the ease with which diffraction patterns of single domains can be obtained by means of the selected area diffraction technique.

2. Experimental method

Alloys were prepared from iodide titanium and high purity TiO_2 within an atmosphere of purified argon in a tungsten-arc furnace. Cast alloys were homogenized at 1200°C for 50 hours prior to heat treatment below the equilibrium temperature (~990°C). Oxygen concentrations were measured by the mass change after combustion in a stream of oxygen at 1200°C. The accuracy of these analyses is estimated as ±0·5 at.% oxygen. Close agreement was obtained by the above method between duplicate analyses and the nominal composition.

Heat treated bulk specimens were polished metallographically to approximately 0·5 mm thickness. Thin foils suitable for electron microscopy were then obtained by chemical polishing at room temperature in a solution containing 33% hydrofluoric acid (40%), 50% nitric acid, and 17% water. A JEM 6A electron microscope was operated at 80 and 100 kV, and both the selected area diffraction and dark field techniques were used.

The interplanar spacings and diffracted intensities were measured on X-ray powder patterns taken with Cu $K\alpha$ radiation. The accuracy of the interplanar spacings was better than 1 part in 1000. However, in the evaluation of the ordered cell parameters a higher accuracy, better than 1 part in 5000, was attained with Co $K\alpha$ and Fe $K\alpha$ radiations in addition to Cu $K\alpha$.

* Present address: Department of Physics, Faculty of Science, Tohoku University, Sendai, Japan.
† Present address: Materials Division, A.A.E.C. Research Establishment, Lucas Heights, Sydney, N.S.W., Australia.

The diffracted intensities were determined by measuring the area under a peak with a planimeter. Partly overlapping reflexions were separated by taking account of the shape of each peak. However, there remained a number of overlapping reflexions containing unresolvable peaks. Since the observed intensities could be strongly influenced by preferred orientation in the powder specimen, the texture of a specimen was examined by an X-ray pole figure method (Schulz, 1949).

3. Results

3.1 *General features*

Specimens quenched from 1500 °C showed no substructure in the electron micrographs, but the electron diffraction patterns contained a distribution of diffuse scattering around the 110 as well as 100 reflexion positions, in addition to the fundamental sharp spots due to the NaCl type structure (Fig. 1). The diffuse scattering is thought to be due to short range order in the arrangement of vacancies. Electron micrographs from specimens annealed at 950 °C for 50 hours, on the other hand, showed an array of small equiaxial regions ($\sim 3\mu$ diameter), each containing one set of parallel bands ($\sim$300–1000 Å wide) (Fig. 2). These specimens gave numerous superlattice spots (Fig. 3) in addition to the fundamental reflexions, but no diffuse scattering. The foil shown in Fig. 2 was approximately parallel to $\{111\}_c$.* It was noted that the position of the fundamental reflexions remained almost unchanged over areas corresponding to the grain size of the disordered phase quenched from high temperatures. The diffraction pattern reproduced in Fig. 3 was obtained from the entire area of Fig. 2, while a simpler diffraction pattern containing fewer superlattice reflexions as shown in Fig. 4 was obtained from the area labelled *A*. Analysis of a number of foils revealed that the boundaries of the bands were parallel to $\{110\}_c$ planes.

3.2 *Construction of the reciprocal lattice*

The following structure analysis is based on the observations of specimens of the equiatomic composition. Typical diffraction patterns from $\{100\}_c$ foils are shown in Fig. 5. The complex pattern in Fig. 5(*a*) containing superlattice reflexions at the 100_c and 110_c positions and also four additional spots around them was obtained from an area including a number of banded regions. With smaller selected areas ($1 \sim 2\mu^2$), however, various types of simpler diffraction pattern were observed. Figs. 5(*b*) and (*c*) contain only the 110_c or 100_c superlattice spots in addition to the fundamental reflexions, and Fig. 5(*d*) contains only half of the spots which were present around the 100_c and 110_c spots in Fig. 5(*a*).

The reciprocal lattice of the ordered structure, shown in Fig. 6, was constructed from electron diffraction patterns of various single orientations obtained by the use of dark field techniques. Figs. 5(*b*), (*c*) and (*d*) correspond respectively to the intensity distribution of the $(010)_c$, $(100)_c$ and $(001)_c$ planes after ordering. A monoclinic cell was chosen to describe the unit cell of this ordered structure. The relationship between the monoclinic axes and the original cubic axes is shown in Fig. 6.

3.3 *Determination of unit cell parameters*

The lattice parameter of the high temperature form of the equiatomic alloy, TiO, was $4{\cdot}1815 \pm 0{\cdot}0005$ Å. After annealing at 950 °C or lower temperatures to some extent, a number of extra reflexions were observed on the X-ray powder pattern. The observed interplanar spacings are shown in Table 1. These spacings are in good agreement with those reported by Andersson, Collen, Kruuse, Kuylenstierna, Magnéli, Pestmalis & Åsbrink (1957).

From a consideration of the interplanar spacings and the relationship between the monoclinic lattice (subscript *m*) and the cubic lattice, as defined in Fig. 6, monoclinic indices were assigned to the X-ray powder reflexions. The parameters of the monoclinic unit cell were evaluated from the following values of $d(hkl)_m$:

$$d(040)_c = d(004)_m = d(4\bar{8}0)_m = 1{\cdot}0355 \pm 0{\cdot}0002 \text{ Å}$$
$$d(2\bar{2}0)_c = d(4\bar{2}0)_m = d(2\bar{4}2)_m = 1{\cdot}4636 \pm 0{\cdot}0003$$
$$d(202)_c = d(222)_m = 1{\cdot}4740 \pm 0{\cdot}0003$$
$$d(220)_c = d(060)_m = 1{\cdot}4845 \pm 0{\cdot}0003 .$$

From these interplanar spacings the parameters of the monoclinic cell were determined to be

$$a = 5{\cdot}855 \pm 0{\cdot}003 \text{ Å}$$
$$b = 9{\cdot}340 \pm 0{\cdot}005$$
$$c = 4{\cdot}142 \pm 0{\cdot}002$$
$$\gamma = 107°32' \pm 3' .$$

The interplanar spacings in this monoclinic lattice are shown in Table 1. The proposed unit cell accounts adequately for all the observed reflexions on the X-ray powder pattern.

As a result of ordering the parent cubic cell ($a_0 = 4{\cdot}1815$ Å) is distorted into a cell with the parameters, $a' = 4{\cdot}2001$, $b' = 4{\cdot}1425$, $c' = 4{\cdot}1420$ Å. An angle between the a' and b' axes is no longer 90° but 89°9′. That is, the parent pseudo-cubic cell has monoclinic symmetry. In § 3.5 the crystallography of ordering will be considered in terms of this pseudo-cubic cell and the subscript c' will be used to indicate Miller indices referred to this basis.

3.4 *Space group and atomic positions*

The electron diffraction spots represented by the reciprocal lattice points shown in Fig. 6 indicate the following systematic absences in the monoclinic unit cell:

$$hkl_m: \; k + l \neq 2n ,$$
$$hk0_m: \; k \neq 2n ,$$
$$00l_m: \; l \neq 2n ,$$

* The subscript *c* will be used to designate Miller indices referred to the cubic axes of the high temperature NaCl type structure of TiO.

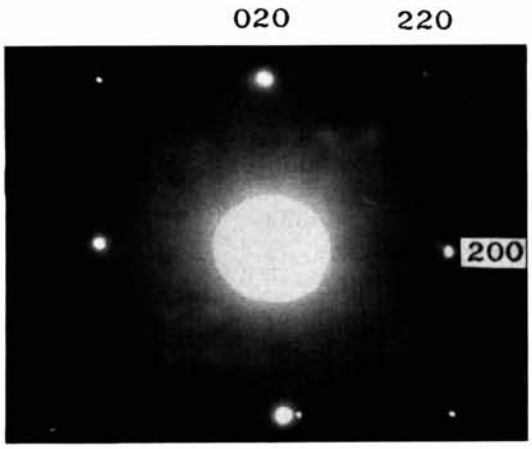

Fig. 1. Electron diffraction pattern of TiO quenched from 1500°C.

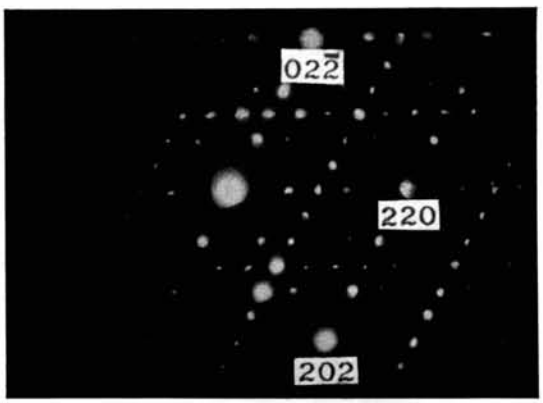

Fig. 3. Diffraction pattern taken from the entire area of Fig. 2. Indices shown in this pattern refer to the high temperature cubic cell.

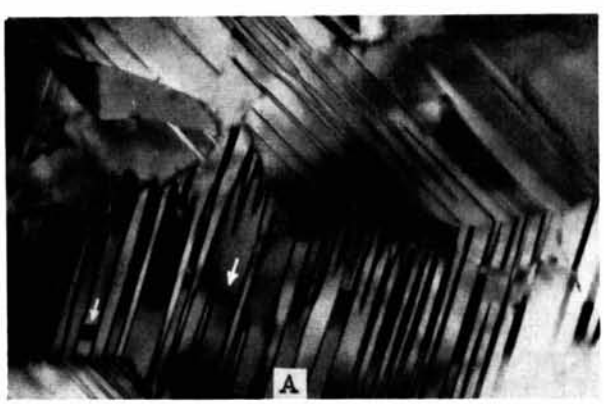

Fig. 2. Electron micrograph of ordered TiO annealed at 950°C for 50 hours. The foil is approximately parallel to $\{111\}_c$ (×40,000).

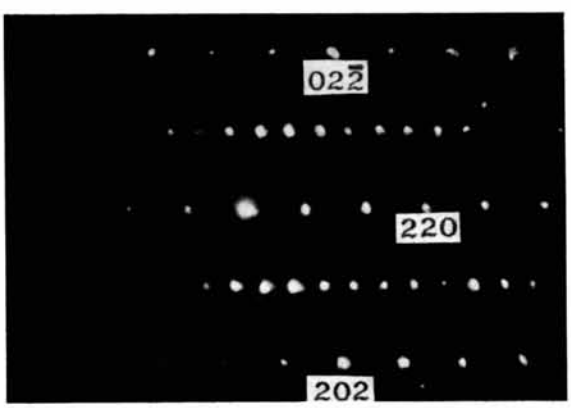

Fig. 4. Diffraction pattern taken from the area labelled *A* in Fig. 2, using a small selected area aperture.

[*To face p.* 308

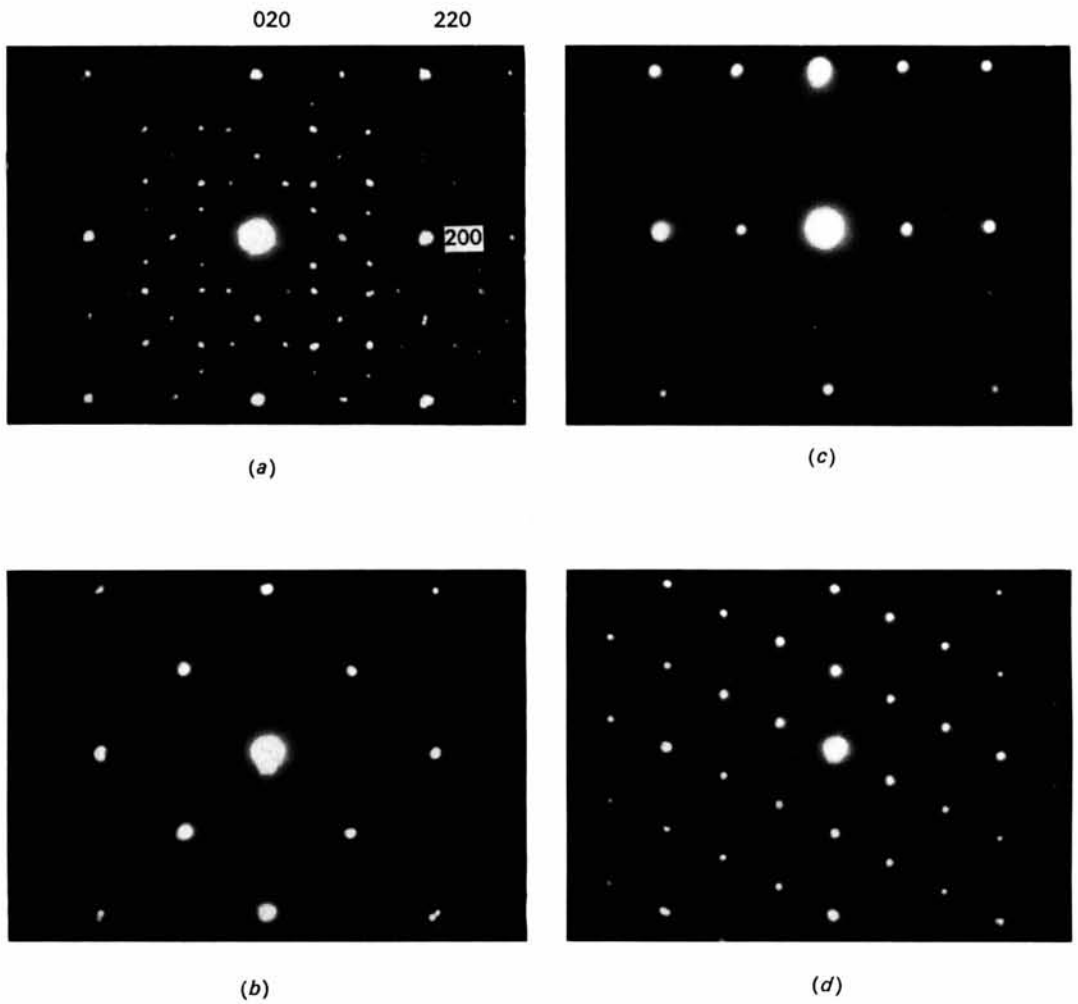

Fig. 5. Diffraction patterns from $\{100\}_c$ foils of ordered TiO annealed at 950 °C for 50 hours; (*b*), (*c*) and (*d*) correspond respectively to the intensity distribution on $(010)_c$, $(100)_c$ and $(001)_c$ planes in the reciprocal lattice shown in Fig. 6, and (*a*) is the superposition of these intensity distributions.

Table 1. *Observed and calculated values of interplanar spacings and* $|F|_{hkl}$

Reflexions without observed values are those which were not detected in the X-ray powder patterns. Values of $|F|_{calc}$ were obtained using parameters calculated from the least-squares refinement discarding $|F|_{obs}$ for unresolvable overlapping peaks (case 1). Reflexions linked together are the unresolvable overlapping reflexions.

hkl_m	d_{calc} (Å)	d_{obs} (Å)	$\|F\|_{obs}$	$\|F\|_{calc}$
100	5·583	5·574	20	20
020	4·453	4·448	21	37
$1\bar{2}0$	4·142	4·137	23	19
011	3·756	3·751	24	23
$1\bar{1}1$	3·317	3·314	33	36
120	3·062	3·061	20	16
111	2·948	2·948	32	37
200	2·792	2·791	38	39
$2\bar{2}0$	2·770	2·771	38	35
$1\bar{3}1$	2·443	2·443	37	41
031	2·413	2·414	64	81
$2\bar{1}1$	2·391	2·391	65	82
$1\bar{4}0$	2·323	—	—	16
040	2·227	2·227	41	37
211	2·116	—	—	18
220	2·098	2·099	207	155
$2\bar{3}1$	2·097		0	0
$2\bar{4}0$	2·071	2·071	197	152
002			197	155
131	2·041	—	—	22
102	1·942	1·942	9	15
$3\bar{2}0$	1·937		17	15
140	1·882	1·881	18	16
022	1·878		9	26
300	1·861	—	—	14
$1\bar{2}2$	1·852	—	—	15
$3\bar{1}\bar{1}$	1·759	1·758	19	27
122	1·715	—	—	14
$1\bar{5}1$	1·702	1·701	25	26
$3\bar{4}0$			49	13
$3\bar{3}1$	1·687	1·687	20	26
202	1·663	1·660	27	28
$2\bar{2}2$	1·659		27	27
231	1·638	1·639	33	18
051	1·637		33	1
$2\bar{5}1$	1·621	1·620	37	33
311	1·590	1·591	25	30
320	1·558	—	—	14
$1\bar{6}0$	1·556	—	—	12
$1\bar{4}2$	1·546	—	—	13
240	1·530	—	—	18
042	1·516	1·517	33	29
$2\bar{6}0$	1·513		15	16
060	1·485	1·485	116	119
222	1·474	1·474	123	121
151	1·465		0	34
$4\bar{2}0$	1·464	1·464	116	119
$2\bar{4}2$			116	119
$3\bar{5}1$	1·443	—	—	18
$3\bar{2}2$	1·415	—	—	13
400	1·396	—	—	20
142	1·393	—	—	14
$4\bar{4}0$	1·385	—	—	19
302	1·384	—	—	12
$3\bar{6}0$	1·381	—	—	16
$4\bar{1}1$	1·366	1·365	16	3
013	1·364		16	15
$1\bar{1}3$	1·340	—	—	21
160	1·338	—	—	11
331	1·325	—	—	23
$3\bar{4}2$	1·315	—	—	11
113	1·310	—	—	22

Table 1 (*cont.*)

hkl_m	d_{calc} (Å)	d_{obs} (Å)	$\|F\|_{obs}$	$\|F\|_{calc}$
$1\bar{7}1$	1·267	1·268	35	11
251			35	59
411	1·257	all overlapped in a flat peak		60
$1\bar{3}3$	1·256			25
340	1·254			12
033	1·252			59
$2\bar{1}3$	1·249			59
322	1·245			11
$1\bar{6}2$	1·244			11
242	1·231	1·231	15	14
420			21	24
$2\bar{6}2$	1·226	—	—	13
071	1·216	1·216	32	27
$4\bar{6}0$			45	22
062	1·206	1·207	75	92
213	1·204	—	—	12
$2\bar{3}3$	1·201	—	—	2
$4\bar{2}2$	1·196	1·195	82	95
133	1·190	—	—	14
260	1·173	—	—	25
$5\bar{2}0$	1·169	—	—	10
$1\bar{8}0$	1·161	—	—	14
$2\bar{8}0$		—	—	24
402	1·158	—	—	16
$3\bar{6}2$	1·149	—	—	13
$3\bar{1}3$	1·125	—	—	17
162	1·124	—	—	9
171	1·123	—	—	18
500	1·117	—	—	11
$3\bar{8}0$	1·115	—	—	8
080	1·113	—	—	7
$1\bar{5}3$	1·110	—	—	17
$5\bar{1}1$	1·109	—	—	17
$3\bar{3}3$	1·106	—	—	16
233	1·092	—	—	11

and the space group $A2/m$ (no. 12 with A, B interchanged) was deduced.

The unit cell of the ordered phase is larger than the high temperature cubic cell and contains twelve titanium and twelve oxygen sites. The proportion of vacancies is estimated to be 16·7% from the density of the ordered structure calculated on the basis of the parameters of the monoclinic unit cell, 5·89 g.cm^{-3}, and the observed pycnometric density, 4·91 g.cm^{-3} (Kuylenstierna & Magnéli, 1956). Intensities of the observed reflexions can approximately be explained if one sixth of both kinds of site are assumed to be vacant, *i.e.* two titanium and two oxygen atoms are missing from the unit cell. The positions of atoms in the proposed structure are as follows:

2Ti in 2(*c*): $\frac{1}{2},0,0$: $\frac{1}{2},\frac{1}{2},\frac{1}{2}$.

2O in 2(*b*): $0,\frac{1}{2},0$: $0,0,\frac{1}{2}$.

4Ti in 4(*i*): $(0,0,0: 0,\frac{1}{2},\frac{1}{2})+x,y,0$: $\bar{x},\bar{y},0$. with $x=\frac{1}{6}$, $y=\frac{1}{3}$.

4Ti in 4(*i*): with $x=\frac{2}{3}$, $y=\frac{1}{3}$.

4O in 4(*i*): with $x=\frac{1}{3}$, $y=\frac{1}{6}$.

4O in 4(*i*): with $x=\frac{5}{6}$, $y=\frac{1}{6}$.

The arrangement of atoms and vacant sites is shown in Fig. 7.

In the absence of intensity measurements on a single crystal, the X-ray powder data were used for the refinement of atomic parameters. This procedure was justified since the $\{200\}_{c'}$ pole figure of the powder specimen showed no evidence of preferred orientation. After correcting for multiplicity and Lorentz–polarization factors the observed intensities were converted into $|F|_{obs}$ values. The reproducibility of the $|F|_{obs}$ values on different samples as well as for repeated diffractometer runs was better than $\pm 10\%$.

The refinement of x and y parameters was carried out by a FORTRAN crystallographic least-squares program, ORFLS, written by Busing, Martin & Levy (1962). The calculations were first performed by discarding $|F|_{obs}$ for unresolvable overlapping reflexions. However, since a number of the strongest reflexions had then to be neglected, the second calculation was made by assuming that the intensities of unresolvable reflexions in an overlapping reflexion were equally divided within it.* Some justification of such an assumption was obtained from the $|F|_{calc}$ values calculated with the parameters derived by the first calculation. For unobserved reflexions, the $|F|_{obs}$ values were calculated by assuming that the intensity of the relevant reflexions was equal to half that of the weakest observed reflexion. Self-consistent field atomic scattering factors were used for oxygen and Thomas–Fermi values for titanium (*International Tables for X-ray Crystallography*, 1962); both atoms were taken to be neutral. An overall isotropic temperature factor, $B=0{\cdot}37$ Å^2, was calculated from the value of the Debye temperature, $\Theta=612$°K, for TiO (Kaufman, 1962).

The parameters of atoms in 4(i) positions after least-squares refinement are shown below. The observed and calculated values of $|F|_{hkl}$ are compared the Table 1.

	Case 1 (Without overlapping peaks)	Case 2 (With overlapping peaks)
4Ti in 4(i) with	$x=0{\cdot}164\pm0{\cdot}005$	$x=0{\cdot}170\pm0{\cdot}004$
	$y=0{\cdot}336\pm0{\cdot}003$	$y=0{\cdot}340\pm0{\cdot}002$
	$z=0$	$z=0$
4Ti in 4(i) with	$x=0{\cdot}666\pm0{\cdot}005$	$x=0{\cdot}669\pm0{\cdot}004$
	$y=0{\cdot}340\pm0{\cdot}002$	$y=0{\cdot}342\pm0{\cdot}002$
	$z=0$	$z=0$
4O in 4(i) with	$x=0{\cdot}324\pm0{\cdot}016$	$x=0{\cdot}343\pm0{\cdot}012$
	$y=0{\cdot}181\pm0{\cdot}009$	$y=0{\cdot}175\pm0{\cdot}007$
	$z=0$	$z=0$
4O in 4(i) with	$x=0{\cdot}819\pm0{\cdot}016$	$x=0{\cdot}833\pm0{\cdot}012$
	$y=0{\cdot}165\pm0{\cdot}010$	$y=0{\cdot}179\pm0{\cdot}008$
	$z=0$	$z=0$

* When there was a superlattice reflexion overlapping fundamental reflexions, all the intensity was assigned to the fundamental reflexions.

The following values of the R index, ($R=\Sigma\,||F|_{obs}-|F|_{calc}|/\Sigma\,|F|_{obs}$), were obtained:

	Case 1	Case 2
Without zeros	0·11	0·16
With zeros	0·19	0·22

3.5 *Microstructural features of the transformation*

In an earlier paper, the present authors (Watanabe, Castles, Jostsons & Malin, 1966) described the microstructural features of the ordered specimen as consisting of small equiaxial domains, each containing one set of parallel plates related to each other by twinning on the $\{110\}_{c'}$ planes.* A more detailed consideration,

* Although, in a cell with monoclinic symmetry, (110), (1$\bar{1}$0), (101), (10$\bar{1}$), (011) and (01$\bar{1}$) planes are no longer equivalent, the expression $\{110\}_{c'}$ will be used here to indicate a set of these planes because the cell designated by the subscript c' is pseudo-cubic. Also $\langle 100\rangle_{c'}$ will be used here to indicate a set of directions, $[100]_{c'}$, $[010]_{c'}$ and $[001]_{c'}$.

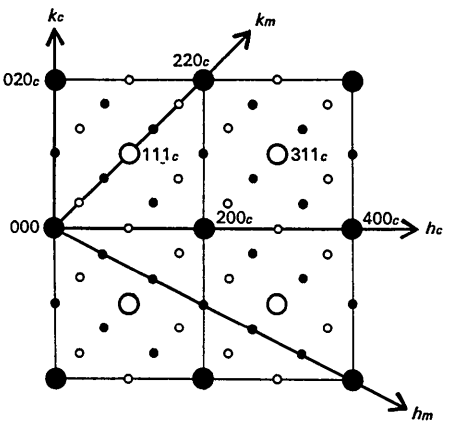

Fig. 6. Reciprocal lattice of ordered TiO. The l axis is perpendicular to the hk plane, and full and open circles represent the reflexions on the $l=0$ plane and on the $l=1$ plane respectively. The subcsripts c and m refer to the original cubic cell and the ordered monoclinic cell respectively.

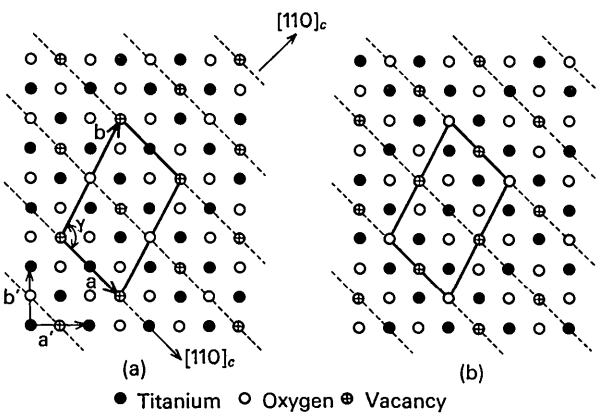

Fig. 7. Structure model of ordered TiO. (*a*) shows the $z=0$ plane and (*b*) shows the $z=\frac{1}{2}$ plane. Thick lines represent the unit cell and dotted lines the planes containing vacancies.

however, has revealed that this simple description should be amended.

The previous analysis was made on area *A* in Fig. 2. From the orientation relation of the image of this area to the corresponding diffraction pattern (Fig. 4), which is shown schematically in Fig. 8, it was concluded that the interface plane of the plates was $\{110\}_{c'}$. Dark field images formed by the superlattice reflexions indicated that the diffraction pattern in Fig. 4 results from the superposition of two sets of spot patterns, one corresponding to the $(\bar{1}11)_{c'}$ plane and the other to the $(\bar{1}1\bar{1})_{c'}$ plane of the reciprocal lattice. In Fig. 8 the open circles represent the superlattice spots of the $(\bar{1}11)_{c'}$ plane and the small full circles represent those on the $(\bar{1}1\bar{1})_{c'}$ plane; the large full circles are the fundamental reflexions common to both reciprocal lattice planes. It can be shown that the alternate plates in this area are related by the twinning elements $(110)_{c'}$, $[\bar{1}10]_{c'}$.

Another example of these microstructural features is shown in Fig. 9(*a*). The foil is again parallel to $\{111\}_{c'}$ and the diffraction pattern taken from a large area containing a number of banded regions is similar to Fig. 3. The dark field images [Fig. 9(*b*) and (*c*)] are complementary with each other in the area labelled *B* of the bright field image. The relationship between the microscope image and the diffraction spots used for the dark field images is shown in Fig. 10, where again the diffraction pattern consists of the superposition of two spot patterns. Fig. 9(*b*) and (*c*) were taken respectively from the spots I and II belonging to the two orientations. By analysis of the orientations (Fig. 10), it is concluded that the superlattice spots represented by small full circles originate from the $(1\bar{1}1)_{c'}$ plates, and those represented by open circles from the $(1\bar{1}\bar{1})_{c'}$ plates. A stereographic analysis showed conclusively that the alternate plates in this area are not twins.

Similar analyses of a large number of electron micrographs have shown that all the $\{110\}_{c'}$ planes can be interface planes. The alternate plates within a domain are twinned only on the $(110)_{c'}$ and $(1\bar{1}0)_{c'}$ interfaces, but not on all other interface planes, *viz.* $(101)_{c'}$, $(10\bar{1})_{c'}$, $(011)_{c'}$, $(01\bar{1})_{c'}$. It is thought, therefore, that these plates may be different crystallographic variants of the cubic to monoclinic transformation. It seems that the twin

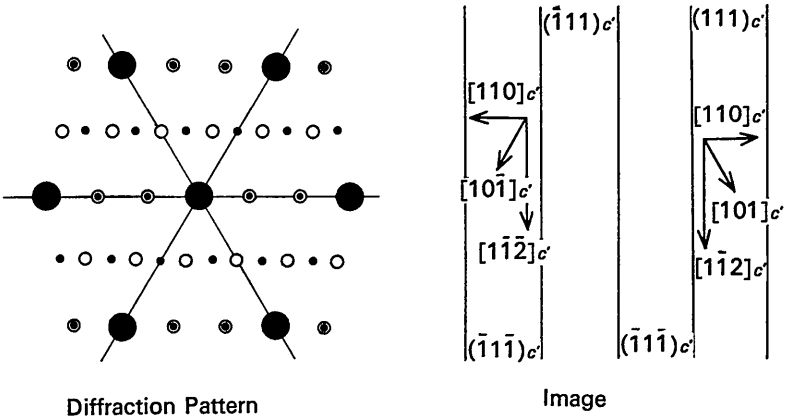

Fig. 8. Correspondence of the diffraction pattern of Fig. 4 to the microscope image of the area *A* in Fig. 2. Large full circles represent the fundamental 220 reflexions. Small full and open circles represent respectively the superlattice spots from the $(\bar{1}1\bar{1})_{c'}$ plates and those from the $(\bar{1}11)_{c'}$ plates in the image.

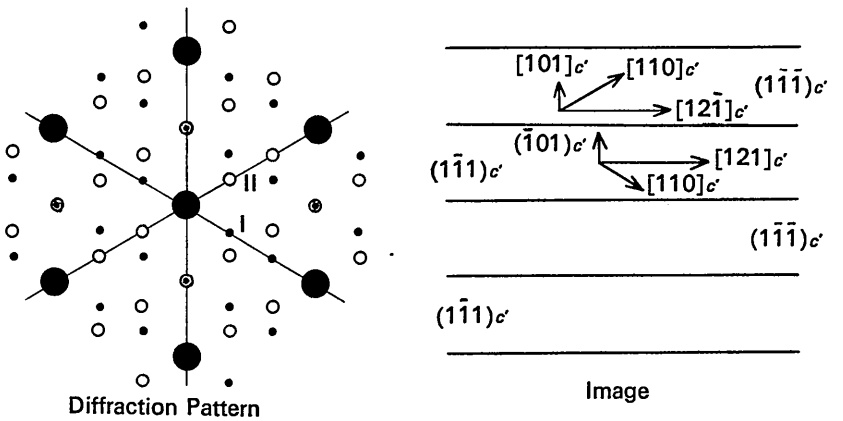

Fig. 10. Correspondence of the microscope image of the area *B* in Fig. 9(*a*) to the diffraction pattern. Small full and open circles represent respectively the superlattice spots from the $(1\bar{1}1)_{c'}$ plates and those from the $(1\bar{1}\bar{1})_{c'}$ plates in the image.

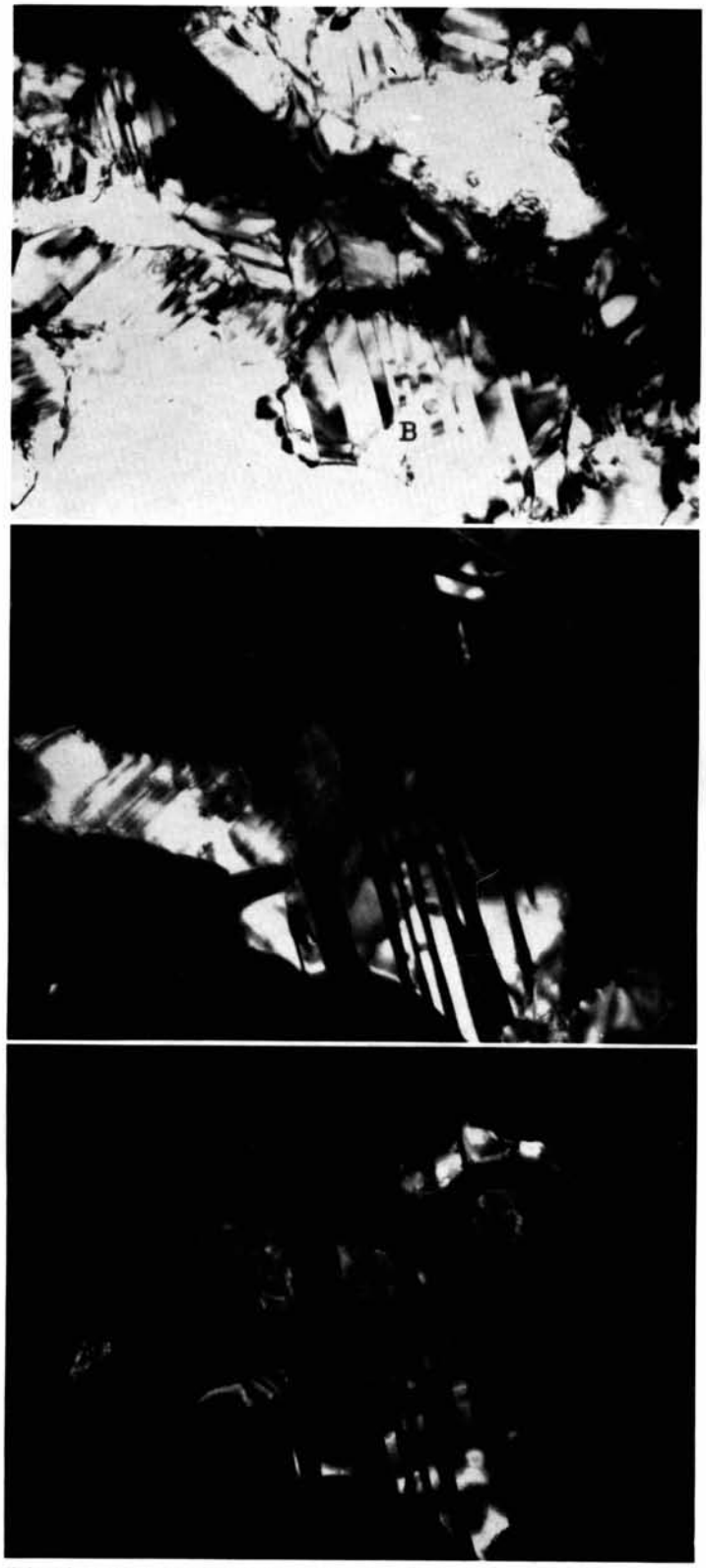

Fig. 9. Electron micrograph of $\{111\}_{fcc}$ foil of ordered TiO. (*a*) is a bright field image, and (*b*) and (*c*) are the corresponding dark field images, taken by using spots I and II, respectively, shown in Fig. 10 ($\times$ 32,000).

[*To face p.* 311

relation between two of the variants is only a fortuitous result of the transformation and is not necessarily a characteristic of the transformation.

The observed crystallographic relationships between neighbouring plates are summarized in Fig. 11. The alternating arrangement of the $\langle 100\rangle_{c'}$ axes in neighbouring plates can be understood in terms of the relative changes of the axial parameters of the high temperature cubic cell on ordering. (The a parameter increases by 0·4% whereas both the b and c parameters decrease by 0·9%). This arrangement seems to occur so as to minimize long range stresses caused by the ordering transformation. When the interface plane is $(011)_{c'}$ or $(01\bar{1})_{c'}$ and the alternating axes are $[010]_{c'}$ and $[001]_{c'}$ the reduction in stress will be small. The rarity of these two as interface planes compared with the other arrangements favours the hypothesis that the requirement of minimum long range stresses has given rise to the observed arrangement of alternating plates.

The observed microstructures can therefore be explained on the basis of the nucleation and growth of the ordered phase within the disordered matrix. The nucleation may occur at many centres on any of the $\{110\}_c$ planes within each grain of the disordered matrix. At any centre of nucleation, a nucleus will grow to form a plate which continues growing until the stress exceeds a critical value, whereupon nucleation and growth of an adjoining plate occurs. This process is repeated until further growth is prevented by the impingement with other sets of plates growing from a neighbouring nucleation centre within the same grain. Thus, each grain of the disordered matrix is subdivided into several domains, each of which contains one set of parallel plates. It is to be emphasized that these domains are not necessarily the antiphase domains commonly found in ordered alloys. In Fig. 2, additional line segments have been observed as shown by the arrows. Their contrast is similar to the image contrast due to the antiphase domain boundaries, but has not been examined in detail in the present investigation.

4. Discussion

The ordered structure of TiO determined in the present investigation can be described in terms of vacancy ordering; *i.e.* in every third (110) plane of the original cubic cell half of the titanium and half of the oxygen atoms are missing alternately. The spacing of this (110) plane is slightly larger than that of the other {110} planes, and as a result, the symmetry of the original cubic structure is reduced to monoclinic. The results of the least-squares refinement have shown that the displacements of the titanium and oxygen atoms from their ideal positions are small in spite of the existence of a large number of vacancies in the crystal. Consideration of the standard error associated with each atomic parameter indicates that there occurs no significant relaxation in positions of the atoms surrounding the vacancies.

Although the proposed ordered structure corresponds to the equiatomic composition TiO, essentially the same structure has been observed in the range of composition $TiO_{0·9}$–$TiO_{1·1}$. Within this composition range there is a change in the number of titanium and oxygen vacancies. This implies that the structure can tolerate some disorder. It is supposed that this disorder can take the form of excess atoms and vacancies which are randomly distributed over the ordered vacant sites and the normally occupied sites, respectively, in the proposed structure.

Another type of ordered structure, which is different from the structure described above, has been observed in alloys near the composition $TiO_{0·7}$ (Watanabe, 1965; Watanabe *et al.*, 1966). The superlattice unit cell, involving six titanium and six oxygen sites, is orthorhombic with the space group $I222$, $a''=a/\sqrt{2}$, $b''=3a/\sqrt{2}$, $c''=a$, where a is the lattice parameter of the original cubic cell. In this alloy there are more oxygen vacancies than titanium vacancies, and the structure results from the ordering of the oxygen vacancies only. All oxygen atoms are missing from every third (110) plane in the original cubic cell, while the titanium vacancies are distributed randomly. It should be noted that this structure was observed only in thin foils annealed at temperatures above 600 °C in the electron microscope or heated by an intense electron beam. The alloy, prior to thinning, was prepared by the diffusion of oxygen into a rolled titanium sheet at 1500 °C. Under equilibrium conditions below 990 °C, this alloy consists of two phases, Ti_2O and the ordered $TiO_{0·9}$ (Jostsons & McDougall, 1967). The orthorhombic structure is, therefore, considered to be a metastable transition phase. This conclusion is supported by the fact that, on the diffraction pattern, diffuse scattering is

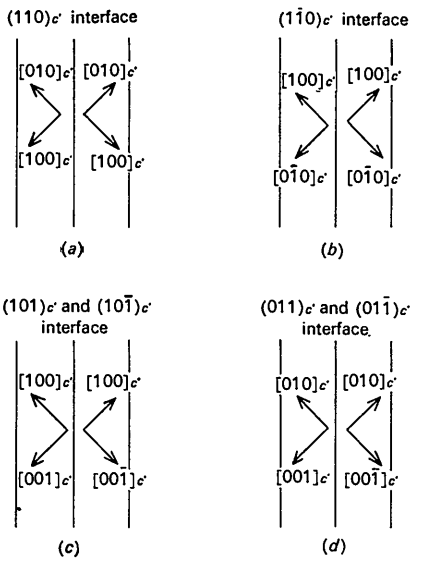

Fig. 11. Schematic representation of the observed crystallographic relationships in the alternating set of plates. Indices refer to the distorted cubic cell, c'.

almost always observed in the positions of the extra spots expected for the equilibrium structure excepting the sharp superlattice spots due to the ordering of oxygen atoms. The diffuse scattering seems to be caused by the short range order of titanium vacancies and it is thought that this transition structure would ultimately transform to the equilibrium ordered structures of $TiO_{0\cdot9}$ and Ti_2O.

Long range order was not observed by previous workers (Andersson, Collen, Kuylenstierna & Magnéli, 1957) in oxygen rich alloys ($TiO_x, x > 1\cdot1$) in which there is an excess of titanium vacancies relative to oxygen vacancies. In the present study, however, diffuse scattering, indicative of the presence of some short range order of vacancies, has been observed in the electron diffraction patterns of an alloy corresponding to $TiO_{1\cdot2}$. This alloy became fully ordered after long annealing treatments below 700 °C but the structure is different from that of the ordered equiatomic alloy. An analysis of this structure is now in progress.

The authors wish to express their sincere thanks to Professors J. M. Cowley and J. S. Bowles for valuable discussions, and to Professor A. E. Jenkins for initiating this work. Grateful acknowledgements are made to the University of Melbourne for the provision of the Sir Thomas Lyle Fellowship in Physics (D.W.) and a research scholarship (J.R.C.) and one of us (D.W.) is indebted to Professor J. M. Cowley for the generous hospitality of his department. The authors (A.J. and A.S.M.) wish to thank Professor H. Muir for the provision of laboratory facilities in the University of New South Wales and to thank the Reserve Bank of Australia for the provision of a scholarship (A.J.). This work was also supported by a research grant from the Australian Institute of Nuclear Science and Engineering.

References

ANDERSSON, S., COLLEN, B., KUYLENSTIERNA, U. & MAGNÉLI, A. (1957). *Acta Chem. Scand.* **11**, 1641.

ANDERSSON, S., COLLEN, B., KRUUSE, G., KUYLENSTIERNA, U., MAGNÉLI, A., PESTMALIS, H. & ÅSBRINK, S. (1957). *Acta Chem. Scand.* **11**, 1653.

BUSING, W. R., MARTIN, K. L. & LEVY, H. A. (1962). Report ORNL-TM-305, Oak Ridge National Laboratory, Tennessee, U.S.A.

EHRLICH, P. (1941). *Z. anorg. Chem.* **247**, 53.

HANSEN, M. (1958). *Constitution of Binary Alloys.* New York: McGraw-Hill.

International Tables for X-ray Crystallography (1962). Vol. III. Birmingham: Kynoch Press.

JENKINS, A. E. (1953). Discussion to paper by Bumps, Kessler & Hansen. *Trans. A.S.M.* **45**, 1025.

JOSTSONS, A. & MCDOUGALL, P. G. (1967). To be published.

KAUFMAN, L. (1962). *Trans. AIME*, **224**, 1006.

KUYLENSTIERNA, U. & MAGNÉLI, A. (1956). *Acta Chem. Scand.* **10**, 1195.

NAYLOR, B. F. (1946). *J. Amer. Chem. Soc.* **68**, 1077.

PEARSON, A. D. (1958). *J. Phys. Chem. Solids*, **5**, 316.

SCHULZ, L. G. (1949). *J. Appl. Phys.* **20**, 1030.

WANG, C. C. & GRANT, N. J. (1956). *Trans. AIME*, **206**, 184.

WATANABE, D. (1965). *Intern. Conf. Electron Diffraction*, Melbourne, 1965, IC-3, Melbourne: Australian Academy of Science.

WATANABE, D., CASTLES, J. R., JOSTSONS, A. & MALIN, A. S. (1966). *Nature, Lond.* **210**, 934.

Acta Cryst. (1967). **23**, 313

The Structure of the Catecholamines. I. The Crystal Structure of Noradrenaline Hydrochloride

BY D. CARLSTRÖM AND R. BERGIN

Department of Medical Physics, Karolinska Institutet, Stockholm 60, *Sweden*

(*Received* 14 *November* 1966)

Crystals of noradrenaline hydrochloride, $C_8H_{11}O_3N.HCl$ are orthorhombic, space group $P2_12_12_1$ with four formula units in a cell having the dimensions $a = 8\cdot580$, $b = 19\cdot120$, $c = 5\cdot775$ Å. The crystal structure has been determined by interpretation of two-dimensional Patterson projections with aid of minimum functions and refined by three-dimensional least-squares methods. The final R index for 1013 observable reflexions is 0·066. The catechol part of the molecule is planar and the bond distances and angles are close to those of tyrosine. As in most chloride salts of organic bases the amine group $\overset{+}{N}H_3$ is hydrogen bonded to Cl^-.

Introduction

Noradrenaline, often also named norepinephrine, which chemically is 1-(3,4-dihydroxyphenyl)-2-aminoethanol, is a hormone serving important physiological functions in endocrine and neural integration. It is released locally by sympathetic nerve endings where it acts as a neurotransmitter but it is also secreted by chromaffin cells, *e.g.* of the adrenal medulla. Since (−)-noradrenaline is of great biological significance we thought it worth while to investigate its crystal structure. To our knowledge, none of the catechol-